Research Article

Electrical, Thermal, and Morphological Properties of Poly(ethylene terephthalate)-Graphite Nanoplatelets Nanocomposites

Basheer A. Alshammari,[1] Arthur N. Wilkinson,[2] and Ghzzai Almutairi[3]

[1]Material Research Institute, King Abdulaziz City for Science and Technology, P.O. Box 6086, Riyadh 11442, Saudi Arabia
[2]Materials Science Centre and North West Composites Centre, School of Materials, The University of Manchester, Grosvenor Street, Manchester M13 9PL, UK
[3]Water and Energy Research Institute, King Abdulaziz City for Science and Technology, P.O. Box 6086, Riyadh 11442, Saudi Arabia

Correspondence should be addressed to Basheer A. Alshammari; bshammari@kacst.edu.sa

Graphite nanoplatelets (GNP) were incorporated with poly(ethylene terephthalate) (PET) matrix by melt-compounding technique using minilab compounder to produce PET-GNP nanocomposites, and then the extruded nanocomposites were compressed using compression molding to obtain films of 1 mm thickness. Percolation threshold value was determined using percolation theory. The electrical conductivity, morphology, and thermal behaviors of these nanocomposites were investigated at different contents of GNP, that is, below, around, and above its percolation threshold value. The results demonstrated that the addition of GNP at loading >5 wt.% made electrically conductive nanocomposites. An excellent electrical conductivity of ~1 S/m was obtained at 15 wt.% of GNP loading. The nanocomposites showed a typical insulator-conductor transition with a percolation threshold value of 5.7 wt.% of GNP. In addition, increasing screw speed enhanced the conductivity of the nanocomposites above its threshold value by ~2.5 orders of magnitude; this behavior is attributed to improved dispersion of these nanoparticles into the PET matrix. Microscopies results exhibited no indication of aggregations at 2 wt.% of GNP; however, some rolling up at 6 wt.% of GNP contents was observed, indicating that a conductive network has been formed, whereas more agglomeration and rolling up could be seen as the GNP content is increased in the PET matrix. These agglomerations reduced their aspect ratio and then reduced their reinforcement efficiency. NP loading (>2 wt.%) increased degree of crystallinity and improved thermal stability of matrix slightly, suggesting that 2 wt.% of GNP is more than enough to nucleate the matrix.

1. Introduction

Graphite nanoplatelets (GNP) are also called expanded graphite (EG) or exfoliated graphite. In graphite form, the graphene sheets are held together by van der Waals interaction which allows some molecules, atoms, or ions to be intercalated between these sheets. Usually, GNP is prepared by modifying graphite using graphite intercalation method (chemical exfoliation method). In this method, graphite is immersed in a concentrated mixture of sulfuric acid with other oxidizers agents. The resulting products are called graphite intercalation compounds (GIC) or expandable graphite. Typically, the GIC materials are heated to a high temperature of ~1000°C for few seconds that generates huge amounts of gases such as sulfur dioxide and water resulting in extra expansion of graphene sheets, which is known as GNP, exfoliated graphite, or expanded graphite (EG). This procedure is achieved under nitrogen or in air atmospheres. Further exfoliation of these materials can produce a single atomic layer of graphite known as graphene. Typically, high ultrasonication process will be used for breaking down the GNP to smaller sheets. Both GIC and GNP are commonly modified graphite forms that have been used for preparing polymer-carbon composites [1–4].

During the previous years, polymer-GNP nanocomposites have been widely investigated to develop materials to be

used where electrical, thermal, and mechanical properties are required. According to a review by Li and Zhong [2] and an investigation study by Alasvand Zarasvand and Golestanian [5], many researchers prepared various conducting polymer nanocomposites containing various GNP weight fractions and sizes under different preparing conditions. Most results indicate significant enhancement in mechanical, thermal, and electrical properties of final nanocomposites. One of the main problems for polymer nanocomposite materials is the appropriate dispersion and distribution of nanofillers into the matrix that needed to be addressed before taking the full advantages of particulate nanoscale fillers.

Furthermore, PET is a thermoplastic polymer. It is used in textile fibers, films, and packaging technologies. This is because PET has good properties such as mechanical and chemical resistance, ability to be spun, and thermal and dimensional stabilities [6, 7].

Despite the above-stated properties, improvement of its electrical conductivity is necessary for electronic applications [8], for example, replacing of indium tin oxide (ITO) electrodes as these materials have poor mechanical and lower conductivity when compared to the conductive carbon nanofillers such as graphene nanoplatelets or carbon nanotubes [2]. The electrical conductivity values higher than 10^{-8} S/m are required for numerous electronic applications, for instance, semiconducting, antistatic, and electromagnetic shielding materials for electronic devices [9].

To achieve electrically conductive pathways within the polymer composites with high conductivity value and acceptable mechanical properties and processability, a reduction of the amount of conductive fillers is required. Therefore, percolation theory is frequently used to determine the percolation threshold value which is the minimum content of conductive fillers associated with the conversion in the electrical behavior of the composite from insulate to conductive phase. This theory also describes the insulator-conductor transitions in polymer composites made of conductive fillers and an insulating polymer matrix. Previous published studies have shown that the percolation threshold value strongly depends on the aspect ratio (length-to-diameter) of the filler particles [10–12].

There are three common adopted methods for the production of composites: solution, in situ polymerization, and melt compounding. The latter method is an environmentally friendly technique. Therefore, it was used in this study. Relatively, there are few investigations reported on PET-GNP nanocomposites. For instance, a study by Zhang et al. [4] prepared PET-GNP nanocomposites using melt blending. A homogenous dispersion of GNP in the PET matrix was noted in this study after some shearing has been used to improve interaction between PET matrix and GNP. Similar work done by Li and Jeong, [8] who prepared PET nanocomposites with diverse concentrations of GNP using melt mixing method, reported good dispersed GNP within the PET matrix, leading to improvements in the mechanical, electrical, and thermal properties of nanocomposites compared with the unfilled PET. The electrical percolation threshold was found to be ~5 wt.% Al-Jabareen et al. [13] added GNP into PET by melt mixing to enhance its oxygen barrier properties. The authors observed a uniform distribution and dispersion of GNP into PET. The results indicated an increase in crystallinity, thermal stability, and Young's modulus of the resultant composite compared to pure PET matrix. However, tensile strength and elongation at break showed reductions of 56% and 40%, respectively. A mother work carried out by Paszkiewicz et al. [14] on the electrical conductivity of PET-GNP nanocomposites prepared by suit polymerization approaches proved good dispersion of GNP in the PET matrix. The transition from insulator to conductor system was started at amount of 0.05 wt.% GNP. Such a low percolation threshold is related to the large surface area, high aspect ratio, and uniform dispersion of the GNP as well as manufacturing method used where monomers polymerized in the existence of the GNP, therefore allowing stronger interactions.

Although the above-mentioned studies have examined properties of PET-GNP nanocomposites, only a few studies have characterized their properties after determining the minimum amount of GNP required for forming conductive pathways within the PET-GNP nanocomposites system. Therefore, in this study, a nanocomposite was prepared using PET as polymer matrix and GNP as nanoscale filler. The effect of GNP on electrical conductivity, morphology, and thermal behavior of PET matrix is investigated as a function of GNP loadings. At first stage of this study, the percolation threshold (Φ_c) value was determined using percolation theory. This value is important for improving fabrication of the polymer composite (PCs) and their properties. The development of PCs based on conductive filler has concentrated on reducing Φ_c in order to reduce cost, improve the fabrication or processability, and enhance mechanical properties of the final composite products [9]. Therefore, finding such value is very important to indicate the performance of the final composite products.

2. Experimental Work

2.1. Materials. PET (matrix) was purchased from Equipolymers Company (Schkopau, Germany) in the form of resin (Grade: LIGHTER C93). It has a glass transition temperature of 75°C, melting temperature of 247°C, and bulk density of 0.88 g/cm^3. XG Sciences, Lansing, MI, USA (xGnPs-15), supplied the GNP (nanoscale filler) in the form of powder. It has average thickness; diameters are ~6–8 nm and 15 μm, respectively.

2.2. Preparation of Nanocomposites. Both as-received materials of PET and GNP dried at about 120°C in vacuum oven overnight before melt compounding was carried out. The PET-GNP nanocomposites were prepared through the melt-compounding technique by mixing or/and compounding PET and GNP in a molten state using a Thermo-Haake Mini-lab compounder. The melt-compounding technique has been described in detail somewhere else [1]. In the current study, the time of mixing was 5 minutes at processing temperature of 280°C and speed of screws was 45 rpm. Then extruded samples were compressed at the same processing temperature, that is, 280°C for 10 min using compression molding machine

and followed by quenching in ice bath to reduce the crystallinity and then chopped, dried at 40°C for 24 h, and stored for the further characterization and testing.

2.3. Characterization of Nanocomposites

2.3.1. Electrical Conductivity and Percolation Threshold Measurements. An impedance spectroscopy, model NumetriQ PSM1735, was used for determining both electrical conductivity values (σ) and percolation threshold values (Φ) for PET and its nanocomposites. Samples plates of dimension (~10 × 10 × 1 mm^3) were cut from compressed films and then coated using sliver paint. The coating is to reduce the contact resistance between the samples and copper wires attached to the specimen using silver epoxy adhesion. Resistance of all tested samples was measured in a range of 1 Hertz up to 10×10^{-6} Hertz at 1 volte as an amplitude voltage. For checking the accuracy, each sample was run five times at room temperature.

2.3.2. Morphology Observations. The morphology state of GNP and the PET nanocomposites was characterized using a SEM (Model: Philips SEM XL30, at an accelerating voltage of 10–20 kV). The nanocomposites were cryogenically frozen in a liquid nitrogen for 5 min and then fractured. The samples were mounted on pin stubs using adhesive tape and then coated with a layer of gold using an Edwards S150B sputter coater, to avoid any charge during scan observation.

TEM (Philips CM200) was applied also at an accelerating voltage of 200 kV. Nanocomposites samples were embedded into epoxy resin for slices purpose using an ultramicrotome and then diamond blade was used to cut slices of ~50 nm thick from the mid of the nanocomposites. In addition, GNP were mixed with ethanol and sonicated using an ultrasonic bath at room temperature for 20 min, and little drops were dropped onto a copper grid using a micropipette. The grid was left to dry in a fume cupboard to evaporate the solvent.

2.3.3. Thermal Behaviors. Crystallization behaviors of PET and its nanocomposites were examined using DSC (TA Instrument DSC Q-100). Samples were scanned from room temperature 270°C under nitrogen condition using a heat-cool-heat run at a heating and cooling rate of 10°C/min. To confirm results, different three specimens of each sample were measured. Thermal stability was investigated using a thermogravimetric analyzer (TGA, TA Q-500). Samples were scanned from room temperature to 700°C under nitrogen and air gas condition.

3. Results and Discussions

3.1. Electrical Conductivity and Percolation Threshold Measurements. From impedance spectroscopy measurements, the σ values are obtained as a function of frequencies. In this study, frequency at 10 Hz has been chosen to obtain the values of σ for comparative purpose for all samples. This is because, at low frequencies, insulator-conductor transitions can be only noticed [11].
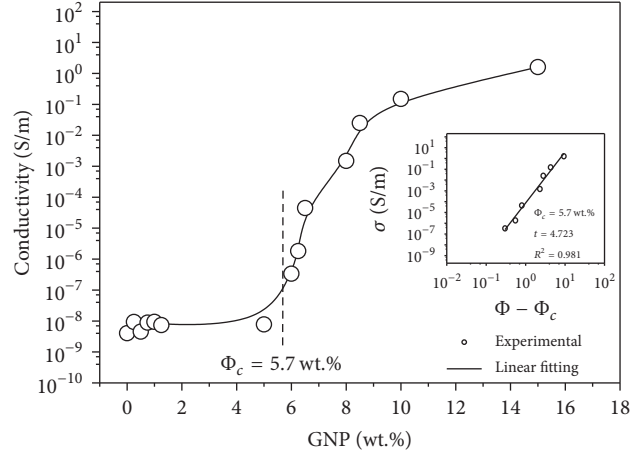

FIGURE 1: Electrical conductivity of PET-GNP nanocomposites. The inset plot is $\log \sigma$ versus $\log (\Phi - \Phi_c)$ for determination of percolation threshold value.

Usually, conductivity values were determined using the following equation [11, 15]:

$$\sigma = \frac{L}{RA}, \tag{1}$$

where σ is the electrical conductivity (S/m), L is the distance between the electrodes (m), A is the cross sectional area (m^2), and R is the measured electrical resistance (Ω).

Figure 1 displays the values of σ of PET matrix and its nanocomposites as a function of GNP loadings. It is clear that σ of the nanocomposites having <5 wt.% of GNP is nearly constant and close to σ of pure PET. Then, a great increase in σ occurs between 5 and 9 wt.% of GNP; this is followed by a small improvement in σ with increasing the amount of GNP. Thus, Φ_c of these nanocomposites is expected between 5 and 9 wt.% loadings of the GNP. Typically, the variation in the conductivity of PCs as a function of the conductive filler content exhibits an S-shaped curve for transition from insolating to conductive system [16]. Therefore, the PET-GNP nanocomposites exhibited a typical transition curve (Figure 1) in this study.

To illustrate transitions of insulator to conductor phase or behavior of PCs reinforced with conductive fillers, percolation theory is applied. This theory will assist the determination of dimensions of conductive network in polymer matrices and percolation threshold values of PCs system. According to this theory, σ of the PCs is calculated by the following equation [11–19]:

$$\sigma = \sigma_o \left(\Phi - \Phi_c\right)^t, \quad \text{for } \Phi > \Phi_c, \tag{2}$$

where σ_o is coefficient constant, Φ_c is percolation threshold value (vol.%), Φ is the filler loading (vol.%), and t is dimension of the conductive network path. In theory, t values of 1.33 and 2.2 represent 2D and 3D systems, respectively. However, experimental values are also stated outside this range somewhere else [17, 18]. The density of the nanofiller (such as GNP) is frequently an approximate value. Therefore, weight fractions have been used for determining the values of Φ_c and
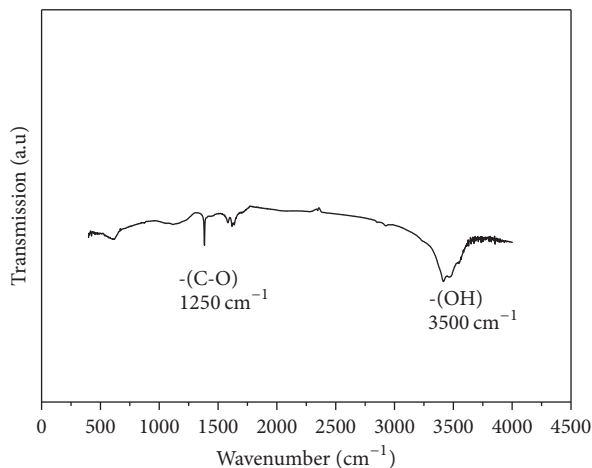
FIGURE 2: FTIR spectra of GNP.

TABLE 1: Electrical conductivity of PET with GNP loading of 5 wt.% and 6 wt.% measured at different processing condition.

Processing conditions	σ at 5 wt.%	σ at 6 wt.%
45 rpm/5 min	7.7×10^{-9}	3.4×10^{-7}
45 rpm/10 min	7.4×10^{-9}	3.2×10^{-7}
90 rpm/5 min	6.8×10^{-9}	3.1×10^{-5}
90 rpm/10 min	7.4×10^{-9}	4.7×10^{-5}

FIGURE 3: FTIR spectra of PET.

t in numerous published studies [12, 15, 16]. In this study, all determinations will be in expression of weight fractions.

According to percolation theory, the best-fit data to the percolation threshold model (2) was achieved at the values of 5.7 wt.% and 4.7 for Φ_c and t, respectively, as shown in the insert graph in Figure 1. These results are in good agreement with the results published in the literature. For example, Zhang et al. [4] obtained a Φ_c at 3.4 vol.% of expanded graphite (~6 wt.%) for PET-expanded graphite nanocomposites using melt-compounding technique. Moreover, Li and Jeong [8] used the same preparation method and reported that the electrical conductive path of exfoliated graphite in the PET matrix was developed at about 5 wt.% of exfoliation graphite filler. These studies reported that there are some functional groups on the surface of the GNP fillers.

Generally, in PCs system, high aspect ratio of such nanofiller is found to reduce Φ_c values. However, based on the data sheets provided by the supplier, the calculated aspect ratio for GNP is ~ 1875. Thus, value of Φ_c is expected to be lower than the value obtained in these studies. The reasons for this could be due to the fact that the GNP has unreduced graphite oxide in the commercial products and then some functional groups are still on its surface after the preparation process. Therefore, FTIR technique was used in the current study to identify the functional groups attached to the surface of GNP during exfoliation techniques (Figure 2). This result is in agreement with those obtained by Li and Jeong [8] who reported some functional groups on the surface of the GNP used. However, a good attraction can occur between the ester groups (-C=O) of PET (see Figure 3) and functional groups such as hydroxyls acids (-OH) on the surface of GNP which leads to improvements in the desperation state of these nanoparticles.

In addition, there is a possibility of an agglomeration and rolling up of GNP filler during melt-compounding process; this could reduce aspect ratio of GNP sheets. Additionally, $t \sim$ 4.72 was much higher than the theoretical values mentioned earlier. Similar value ($t \sim 4.25$) has been obtained by Zhang et al. [4] for PET-EG nanocomposites. The authors proposed the reasons for this deviation, that is, tunneling transmission, the microstructure, and anisotropic behavior of the composites.
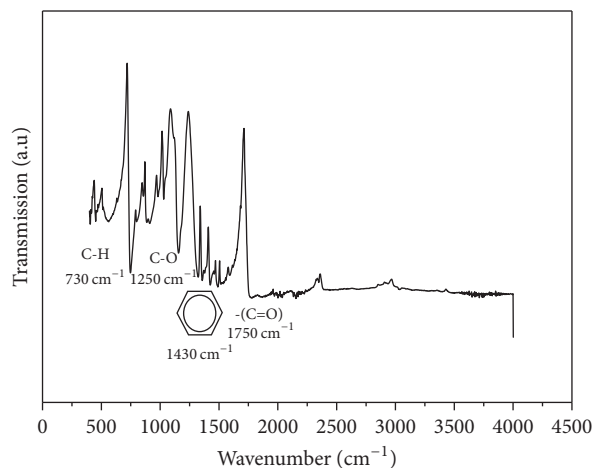
Additionally, the screw speed and residence time during melt process are expected to impact the values of σ of PCs [20, 21]. Therefore, in the present study, the impact of these two processing parameters on σ was investigated. Two samples were selected just before and after ϕ_c value of the nanocomposites to note the effect of processing parameter on its conductivity.

Table 1 shows σ data for the nanocomposites processed at two different screw speeds and residence times. It is clear that the screw speed has an important effect on σ for the samples above that of ϕ_c only, where σ increased by ~2.5 orders of magnitude for the nanocomposites processed at 90 rpm instead of 45 rpm. In contrast, there is no obvious effect of screw speed for samples having loading below ϕ_c. This could be due to the amount of GNP being insufficient to form a conductive path whatever its dispersion state in the composite. In contrast, increasing the residence time of the nanocomposites mixing from 5 to 10 minutes had no important effect on their electrical conductivity.

3.2. Morphological Characterization. The morphology of GNP was examined before its incorporation into the PET matrix in order to understand their size and shapes. Figure 4 shows SEM image of as-received GNP. As can be seen, it shows the separated platelets resulting from break down of expandable graphite particles during the preparation process of GNP [22].

Similar morphologies for GNP were observed in previous studies [8, 22, 23]. On the other hand, Figures 5, 6, and 7 show the PET-GNP nanocomposites at 2, 6, and 8 wt.% of GNP loading. The nanocomposites at 2 wt.% of GNP show uniform

TABLE 2: DSC data for PET-GNP nanocomposites.

GNP (wt.%)	T_{cc} (°C)	T_{m1} (°C)[*]	T_{m2} (°C)[**]	T_{mc} (°C)	X_c (%)[***]
0	133.6 ± 0.2	253.4 ± 0.4	245.9 ± 0.9	209.2 ± 0.1	11.8 ± 1.8
2	120.1 ± 0.3	253.8 ± 0.5	247.1 ± 1.0	220.0 ± 0.2	19.3 ± 0.3
4	118.8 ± 0.7	251.5 ± 0.4	248.3 ± 1.7	219.9 ± 0.2	19.6 ± 2.4
6	116.6 ± 0.2	251.2 ± 1.0	248.8 ± 0.5	220.7 ± 0.4	21.1 ± 1.3
8	114.7 ± 0.3	251.9 ± 1.4	249.2 ± 0.3	220.9 ± 0.7	22.0 ± 1.8
10	114.7 ± 1.2	251.5 ± 0.4	249.3 ± 0.5	220.7 ± 0.6	22.4 ± 0.6

[*]Melting temperatures values obtained from the first heating runs. [**]Melting temperatures values obtained from the second heating runs. [***]Degree of crystallinity after quenching process ($X_c = X_m − X_{cc}$), where X_m is crystallinity related to melting processes and X_{cc} is crystallinity linked with cold crystallization process.
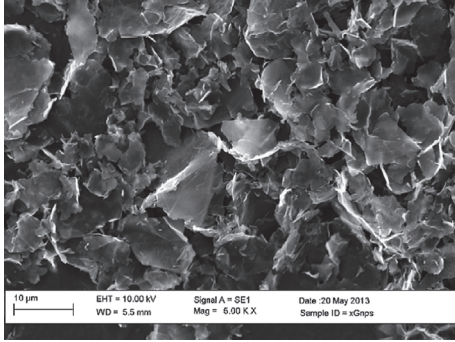
FIGURE 4: SEM image of GNP.

distribution and no sign of aggregations/agglomeration (Figure 5). Nevertheless, at higher GNP loadings, the aggregation and rolling up of GNP are observed.

For instance, the nanocomposites containing 6 wt.% of GNP, which are just above Φ_c, showed some rolling up and agglomeration (Figure 6), indicating that a conductive network has been formed which allows the electron to move.

More agglomeration could be observed in Figure 7 as the GNP content is increased. Similar morphology observations have been reported for polypropylene nanocomposites by Kalaitzidou et al. [24]. In addition, Zhang et al. [4] considered the relationship between the morphology and σ of PET-EG nanocomposites. In the SEM results, it has been observed that when adding EG above Φ_c, particles contacted with each other, indicating that conductive path has been developed. However, below Φ_c, the conductive particles were observed far away from each other; thus, there is no path for electron to move in the nanocomposite system.

Figure 8 shows the TEM images of both pure GNP and PET-GNP nanocomposites. The folding and rolling up of nanoplatelets in the composite are clearly observed. Similar observations have been reported by Kalaitzidou et al. [24] for same grade of GNP in a PP matrix.

3.3. Thermal Analyses of PET-GNP Nanocomposites

3.3.1. Crystallization Behavior. Pure PET and the nanocomposites with varying contents of GNP (2, 4, 6, 8, and 10 wt.%) were exposed to heat/cool/heat cycles at heating and cooling of 10°C/min. The DSC curves in Figures 9(a)–9(d) show cold crystallization peaks, melting peaks from the first run, melt crystallization peaks, and melting peaks from the second

cycle, respectively. The data obtained from these peaks are presented in Table 2.

From Figure 9(a) and Table 2, it is clear that the incorporation of 2 wt.% GNP into PET matrix decreased the cold crystallization temperature (T_{cc}) by 14°C, followed by slight decrease in T_{cc} with increasing GNP loadings. This reduction in the value of T_{cc} indicates that the cold crystallization of the nanocomposites was initiated earlier than that of pure PET matrix. During the cooling run (Figure 9(c)), the PET-GNP nanocomposites displayed roughly 10°C higher melt crystallization temperature (T_{mc}) than pure PET (Table 2). In addition, degree of supercoiling is ($T_m − T_{mc}$), where T_m is melting temperature. This difference in temperatures reflects the rate of crystallization. From Table 2, it is clear that ($T_m − T_{mc}$) decreased with increasing amount of GNP. It should be noted that addition of >2 wt.% of GNP results only in slight changes in the values of T_{cc}, T_{mc}, and ($T_m − T_{mc}$), indicating that 2 wt.% loading of GNP is more than enough to nucleate the PET matrix. Such an effect in the crystallizations of PET is in agreement with previous work done by [25, 26].

X_c can be calculated using the enthalpies of both crystallization and melting, according to the following equation [27, 28]. X_c of PET and its nanocomposite was calculated from the first-heat run as these data reflect the thermal history of the samples.

$$X_C = \frac{\Delta H_m − \Delta H_{cc}}{\left(1 − w_f\right)\Delta H_o} * 100, \tag{3}$$

where ΔH_m is the melting enthalpy (J/g), ΔH_{cc} is the cold crystallization enthalpy (J/g), ΔH_o is the theoretical enthalpy of 100% crystalline PET ($\Delta H_o = 140$ J/g) [26], and w_f is the weight fraction of GNP.

The addition of GNP was found to affect X_c as presented in Table 2. There is an improvement of ~7.5% in the value of X_c upon adding of 2 wt.% of GNP. However, additional adding of GNP does not show any considerable alteration in the values of X_c. Similar behavior was observed by Al-Jabareen et al. [13], who studied PET-GNP nanocomposites and reported an enhancement of 4% in value of X_c at 1.5 wt.% GNP concentration. In contrast, it was reported that GNP did not change the values of X_c of a PP matrix [25].

Furthermore, the addition of GNP appears to have no noticeable effect on values of T_m within the content of GNP used in this study (Table 2). Comparative peaks of melting for two the heating runs are shown in Figures 9(b) and 9(d). From these curves and Table 2, it can be observed that the
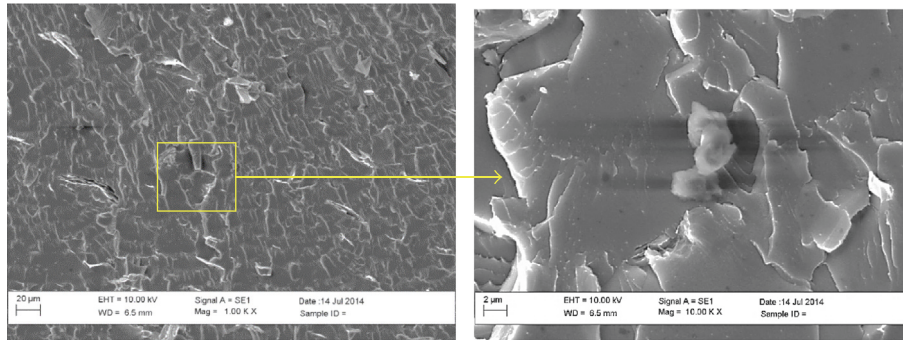
FIGURE 5: SEM images at low and high magnifications of fracture surfaces of PET-GNP nanocomposites containing 2 wt.% of GNP.
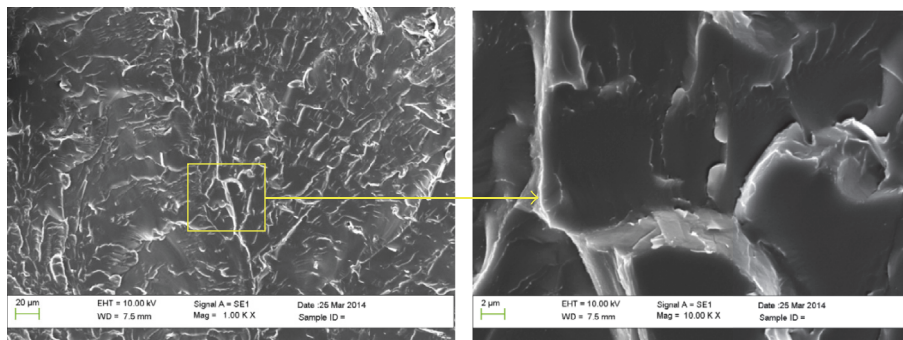

FIGURE 6: SEM images at low and high magnifications of fracture surfaces of PET-GNP nanocomposites containing 6 wt.% of GNP.
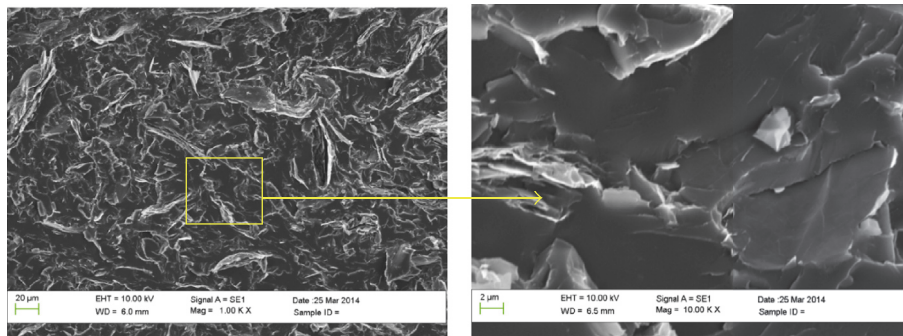

FIGURE 7: SEM images at low and high magnifications of fracture surfaces of PET-GNP nanocomposites containing 8 wt.% of GNP.
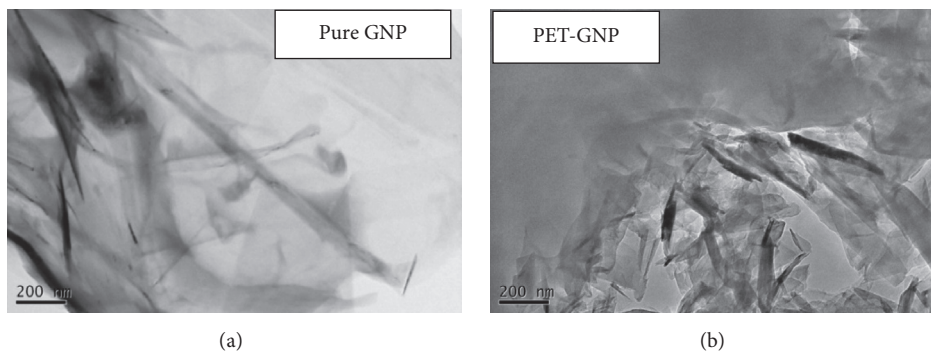

(a)

(b)

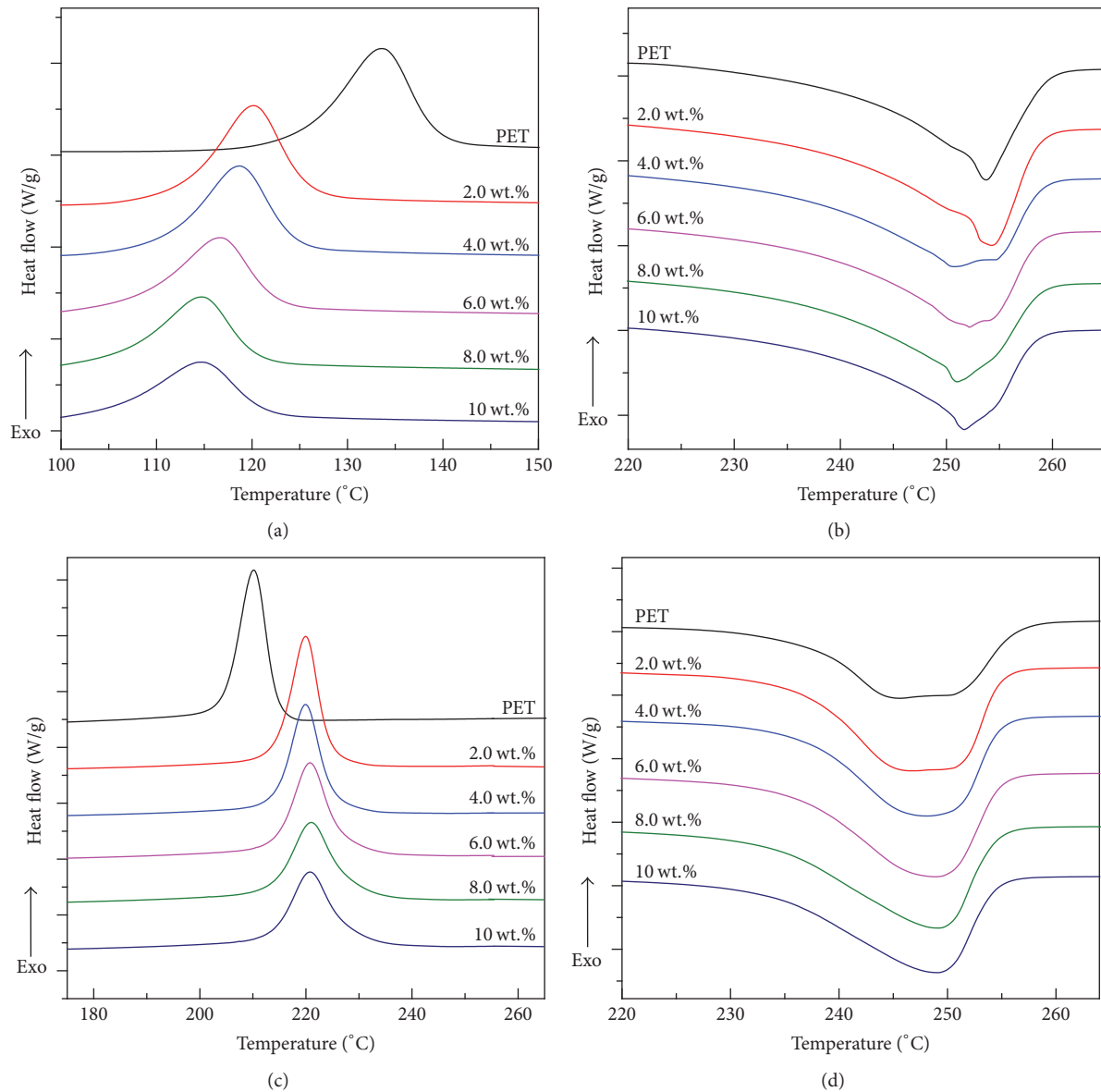FIGURE 8: TEM images of as-received GNP (a) and a PET-GNP nanocomposite containing 6 wt.% of GNP (b).

FIGURE 9: DSC curves of PET-GNP nanocomposites showing cold crystallization peaks (a), melting peaks from the first scan (b), subsequent cooling curves (c), and melting peaks from second heating run (d).

values of T_{m2} are lower than that of T_{m1}. Similar observations were reported by Kalaitzidou et al. [25] who studied the nucleation effects and crystallization behavior of polypropylene- (PP-) GNP nanocomposites. They observed that GNP changed the melting behavior of PP matrix. This behavior was attributed to both the increased homogeneity and thinning of crystal size.

3.3.2. Thermal Stability. Modified graphite forms such as GNP have been used to improve thermal stability of polymer matrices. For example, Al-Jabareen et al. [13] reported that the adding of GNP into PET matrix delays the onset temperature of degradation, indicating the improvement of thermal stability. The authors attributed this improvement to 2D structure of GNP that acts as barrier for oxygen diffusion through

the nanocomposites. A similar result was given by Li and Jeong [8]. In other studies, thermal stability enhancements have been reported for polycarbonate-GNP nanocomposites [29] and poly(methyl methacrylate) as a polymer matrix [30] using the same grade of GNP as used in the current study.

The results of the present study agree with these studies; as in the current work, the incorporation of GNP into PET matrix enhanced its thermal stability of PET under nitrogen and air as shown in Figures 10 and 11, respectively. $T_{5\%}$ values taken from these curves are presented in Table 3. It is clear that the values of $T_{5\%}$ for the nanocomposites are higher than that of pure PET in both atmospheres, indicating that GNP enhanced the thermal stability. $T_{5\%}$ values for neat PET are $\approx 382°C$ and $\approx 370°C$ in nitrogen and air, respectively. However, $T_{5\%}$ values for the nanocomposites having 2 wt.%
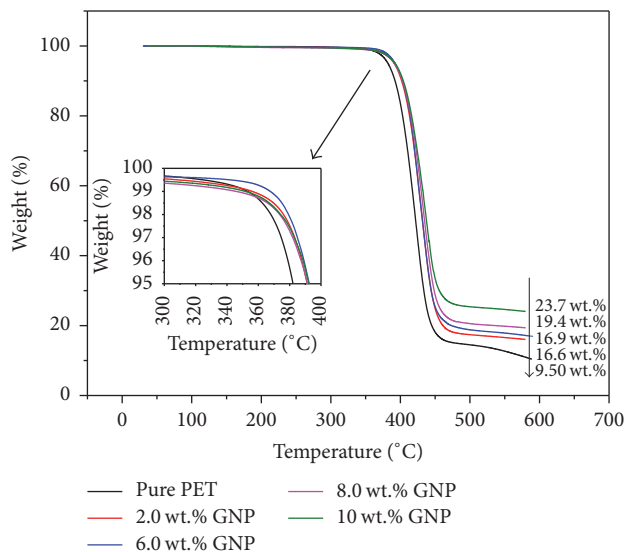
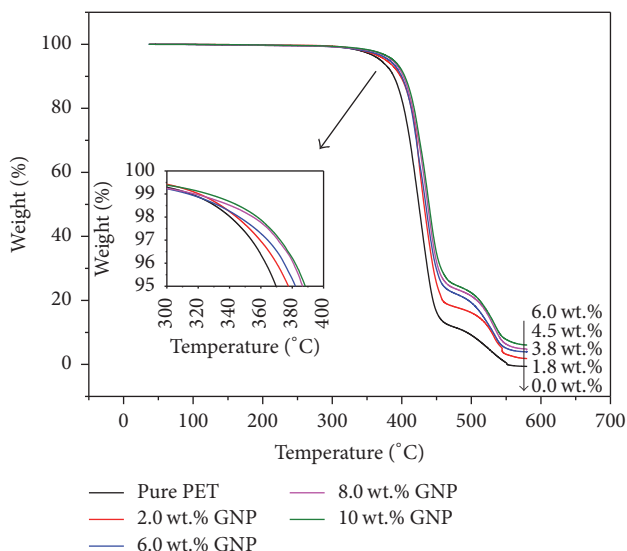FIGURE 10: TGA thermograms of nanocomposites examined under nitrogen atmosphere.

FIGURE 11: TGA thermograms of nanocomposites examined under air atmosphere.

GNP are ~392°C and ~378°C in nitrogen and air, respectively. Addition of >2 wt.% GNP improved the thermal stability slightly. This could be due to the agglomeration and rolling up of GNP during melt mixing at higher loadings.

Furthermore, pure PET and the nanocomposites have lower $T_{5\%}$ values when heated in air (Figure 11) compared with when heated in nitrogen. However, the improvement of $T_{5\%}$ values in air is higher than that in nitrogen when compared to pure PET. For example, with the addition of 10 wt.% of GNP, $T_{5\%}$ values are higher than unfilled PET matrix by ~11°C and ~18°C in nitrogen and air atmospheres, respectively (Table 3).

The enhanced thermal stabilities in the previous studies explained by a barrier effect associated with GNP filler that

TABLE 3: Thermal degradation temperatures (T_5%) for PET-GNP nanocomposites under nitrogen and air atmospheres.

GNP (wt.%)	N$_2$ $T_{5\%}$ (°C)	Air $T_{5\%}$ (°C)
0	382.0 ± 1.4	370.0 ± 1.0
2	391.9 ± 1.3	378.2 ± 0.5
6	393.2 ± 1.3	384.9 ± 3.0
8	392.3 ± 1.1	386.9 ± 0.7
10	393.1 ± 0.9	388.5 ± 0.1

obstructs the diffusion of oxygen into the nanocomposites and hinders diffusion of volatiles materials.

4. Conclusion

In the present study, a large number of nanocomposites were prepared using PET matrix and GNP nanofiller by melt-compounding method in order to determine the percolation threshold value for PET-GNP nanocomposites system. The electrical conductivity, morphology, thermal stability, crystallization behaviors, and degree of crystallinity of these nanocomposites were characterized. In particular, at ~6 wt.% of GNP, an enhancement in conductivity was observed. Such loading marks the insulator-conductor transition having a percolation threshold value of 5.7 wt.%. The conductivity that is required for antistatic applications was observed just above the percolation threshold value. Screw speed during mixing exhibited strong influence on the conductivity of the nanocomposites above such value. Addition of ~2 wt.% GNP into PET matrix caused an increase in the degree of crystallinity, accelerating both cold and melt crystallizations along with good improvements in the thermal stability. However, further addition (>2 wt.%) improves thermal properties slightly. This attributed to higher agglomeration, pulling out, and rolling up of GNP sheets during mixing process, which reduced their aspect ratio and then reduced reinforcement efficiency.

Conflicts of Interest

The authors declare that there are no conflicts of interest regarding the publication of this paper.
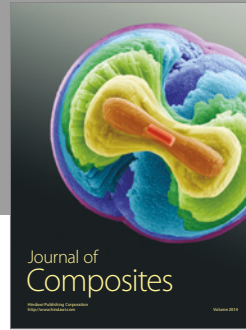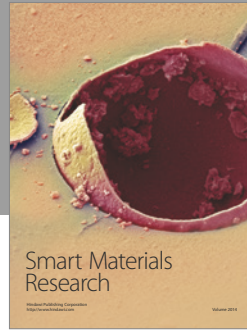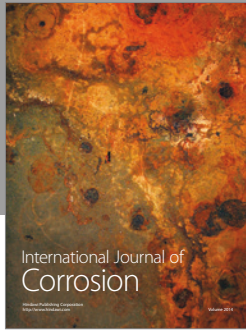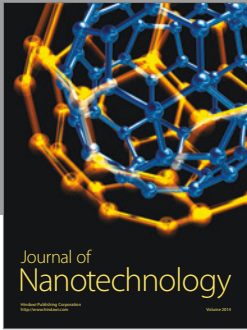
Acknowledgments

References

[1] R. Sengupta, M. Bhattacharya, S. Bandyopadhyay, and A. K. Bhowmick, "A review on the mechanical and electrical properties of graphite and modified graphite reinforced polymer composites," *Progress in Polymer Science (Oxford)*, vol. 36, no. 5, pp. 638–670, 2011.

[2] B. Li and W.-H. Zhong, "Review on polymer/graphite nano-platelet nanocomposites," *Journal of Materials Science*, vol. 46, no. 17, pp. 5595–5614, 2011.

[3] M. Li and Y. G. Jeong, "Influences of exfoliated graphite on structures, thermal stability, mechanical modulus, and electrical resistivity of poly(butylene terephthalate)," *Journal of Applied Polymer Science*, vol. 125, no. 1, pp. E532–E540, 2012.

[4] M. Zhang, D.-J. Li, D.-F. Wu, C.-H. Yan, P. Lu, and G.-M. Qiu, "Polyethylene terephthalate/expanded graphite conductive composites: Structure, properties, and transport behavior," *Journal of Applied Polymer Science*, vol. 108, no. 3, pp. 1482–1489, 2008.

[5] K. Alasvand Zaravand and H. Golestanian, "Investigating the effects of number and distribution of GNP layers on graphene reinforced polymer properties: Physical, numerical and micromechanical methods," *Composites Science and Technology*, vol. 139, pp. 117–126, 2017.

[6] J. Brydson, *Plastic Materials*, Butterworth-Heineman Linacre House, Oxford, UK, 1999.

[7] C. A. Harper and E. M. Petrie, *Plastics Materials and Processes: a Concise Encyclopedia*, John Wiley & Sons, 2003.

[8] M. Li and Y. G. Jeong, "Poly(ethylene terephthalate)/exfoliated graphite nanocomposites with improved thermal stability, mechanical and electrical properties," *Composites Part A: Applied Science and Manufacturing*, vol. 42, no. 5, pp. 560–566, 2011.

[9] P.-C. Ma, N. A. Siddiqui, G. Marom, and J.-K. Kim, "Dispersion and functionalization of carbon nanotubes for polymer-based nanocomposites: a review," *Composites A: Applied Science and Manufacturing*, vol. 41, no. 10, pp. 1345–1367, 2010.

[10] F. Xin, L. Li, S. H. Chan, and J. Zhao, "Influences of carbon fillers on electrical conductivity and crystallinity of polyethylene terephthalate," *Journal of Composite Materials*, vol. 46, no. 9, pp. 1091–1099, 2012.

[11] Z. Římská and V. Křesálek, "AC conductivity of carbon fiber - polymer matrix," *Polymer Composites*, vol. 23, 2002.

[12] J. K. W. Sandler, J. E. Kirk, I. A. Kinloch, M. S. P. Shaffer, and A. H. Windle, "Ultra-low electrical percolation threshold in carbon-nanotube-epoxy composites," *Polymer*, vol. 44, no. 19, pp. 5893–5899, 2003.

[13] A. Al-Jabareen, H. Al-Bustami, H. Harel, and G. Marom, "Improving the oxygen barrier properties of polyethylene terephthalate by graphite nanoplatelets," *Journal of Applied Polymer Science*, vol. 128, no. 3, pp. 1534–1539, 2013.

[14] S. Paszkiewicz, A. Szymczyk, M. Soccio, J. Mosnáček, T. A. Ezquerra, and Z. Rosłaniec, "Electrical conductivity of poly(ethylene terephthalate)/expanded graphite nanocomposites prepared by *in situ* polymerization," *Journal of Polymer Science, Part B: Polymer Physics*, vol. 50, no. 23, pp. 1645–1652, 2012.

[15] J. Sandler, M. S. P. Shaffer, T. Prasse, W. Bauhofer, K. Schulte, and A. H. Windle, "Development of a dispersion process for carbon nanotubes in an epoxy matrix and the resulting electrical properties," *Polymer*, vol. 40, no. 21, pp. 5967–5971, 1999.

[16] M. L. Clingerman, E. H. Weber, J. A. King, and K. H. Schulz, "Development of an additive equation for predicting the electrical conductivity of carbon-filled composites," *Journal of Applied Polymer Science*, vol. 88, no. 9, pp. 2280–2299, 2003.

[17] J. O. Aguilar, J. R. Bautista-Quijano, and F. Avilés, "Influence of carbon nanotube clustering on the electrical conductivity of polymer composite films," *Express Polymer Letters*, vol. 4, no. 5, pp. 292–299, 2010.

[18] R. J. Young and P. A. Lovell, *Introduction to Polymers*, CRC Press, Boca Raton, Fla, USA, 3rd edition, 2011.

[19] W. Bauhofer and J. Z. Kovacs, "A review and analysis of electrical percolation in carbon nanotube polymer composites," *Composites Science and Technology*, vol. 69, no. 10, pp. 1486–1498, 2009.

[20] M. Guehenec, V. Tishkova, S. Dagreou et al., "The effect of twin screw extrusion on structural, electrical, and rheological properties in carbon nanotube poly-ether-ether-ketone nanocomposites," *Journal of Applied Polymer Science*, vol. 129, no. 5, pp. 2527–2535, 2013.

[21] T. Villmow, P. Pötschke, S. Pegel, L. Häussler, and B. Kretzschmar, "Influence of twin-screw extrusion conditions on the dispersion of multi-walled carbon nanotubes in a poly(lactic acid) matrix," *Polymer*, vol. 49, no. 16, pp. 3500–3509, 2008.

[22] S. Kim, J. Seo, and L. T. Drzal, "Improvement of electric conductivity of LLDPE based nanocomposite by paraffin coating on exfoliated graphite nanoplatelets," *Composites Part A: Applied Science and Manufacturing*, vol. 41, no. 5, pp. 581–587, 2010.

[23] M. Li and Y. G. Jeong, "Preparation and characterization of high-performance poly(trimethylene terephthalate) nanocomposites reinforced with exfoliated graphite," *Macromolecular Materials and Engineering*, vol. 296, no. 2, pp. 159–167, 2011.

[24] K. Kalaitzidou, H. Fukushima, and L. T. Drzal, "A route for polymer nanocomposites with engineered electrical conductivity and percolation threshold," *Materials*, vol. 3, no. 2, pp. 1089–1103, 2010.

[25] K. Kalaitzidou, H. Fukushima, P. Askeland, and L. T. Drzal, "The nucleating effect of exfoliated graphite nanoplatelets and their influence on the crystal structure and electrical conductivity of polypropylene nanocomposites," *Journal of Materials Science*, vol. 43, no. 8, pp. 2895–2907, 2008.

[26] J.-Z. Xu, G.-J. Zhong, B. S. Hsiao, Q. Fu, and Z.-M. Li, "Low-dimensional carbonaceous nanofiller induced polymer crystallization," *Progress in Polymer Science*, vol. 39, no. 3, pp. 555–593, 2014.

[27] S. Yesil and G. Bayram, "Poly(ethylene terephthalate)/carbon nanotube composites prepared with chemically treated carbon nanotubes," *Polymer Engineering and Science*, vol. 51, no. 7, pp. 1286–1300, 2011.

[28] G. Antoniadis, K. M. Paraskevopoulos, D. Bikiaris, and K. Chrissafis, "Melt-crystallization mechanism of poly(ethylene terephthalate)/multi-walled carbon nanotubes prepared by in situ polymerization," *Journal of Polymer Science, Part B: Polymer Physics*, vol. 47, no. 15, pp. 1452–1466, 2009.

[29] G. Gedler, M. Antunes, V. Realinho, and J. I. Velasco, "Thermal stability of polycarbonate-graphene nanocomposite foams," *Polymer Degradation and Stability*, vol. 97, no. 8, pp. 1297–1304, 2012.

[30] T. Ramanathan, S. Stankovich, D. A. Dikin et al., "Graphitic nanofillers in PMMA nanocomposites—an investigation of particle size and dispersion and their influence on nanocomposite properties," *Journal of Polymer Science Part B: Polymer Physics*, vol. 45, no. 15, pp. 2097–2112, 2007.